Estimate of the Tropospherical Water Vapor Through Microwave Attenuation Measurements in Atmosphere

Fabrizio Cuccoli and Luca Facheris

***Abstract*—The objective of this paper is to proceed, by investigating the statistics of simulated measurements based on a large dataset of radiosonde profiles, to assess the feasibility of active systems providing water vapor profile information based on Earth-satellite multifrequency differential attenuation measurements made in the 18–22-GHz range. Recently, in fact, we pointed out the potential and the advantages of such measurements, showing in particular how a spectral sensitivity parameter could be exploited to provide the total water vapor content and further information about the shape of its vertical profile. In this work, we present an in-depth statistical analysis of the relationship between the spectral sensitivity parameter and the water vapor content at different tropospheric layers. Furthermore, we discuss the performance of a simple amplitude modulation transmit–receive system that could be adopted to provide the sensitivity measurements. It is shown that a dual-frequency system can directly provide with good accuracy the columnar water vapor content separately from the content of the 3–9 km atmospheric layer.**

***Index Terms*—Attenuation measurements, radiosondes, spectral analysis, vertical profiles, water vapor.**

I. Introduction

RECENTLY, we presented a detailed spectral analysis of the atmospheric attenuation effects generated by vertical profiles of water vapor around the 22.235 GHz absorption line [1]. The motivation was the exploitation of active systems at microwaves based on attenuation measurements, potentially allowing significantly better SNR, spectral, and radiometric resolution than conventional radiometers. The objective was to investigate how water vapor profiles are correlated to the spectral attenuation characteristics of the atmosphere along an active Earth-satellite link. The approach proposed was based on multifrequency differential attenuation measurements made by a transmitter–receiver pair along such a link. The greater variations with frequency of the absorption characteristics of water vapor with respect to the other atmospheric components make the differential approach adequate for evidencing the attenuation contribution by water vapor. The conclusion of the analysis, which accounted for uncertainties due to variations of temperature and pressure profiles, was that the differential approach could be usefully exploited to define a spectral sensitivity function carrying information about the vertical profiles of water vapor.

Manuscript received August 13, 2001; revised January 3, 2002. This work was supported by the Italian Space Agency and by the Italian Ministry for Technological and Scientific Research.

The authors are with the Dipartimento di Elettronica e Telecomunicazioni, Università di Firenze, 50139 Firenze, Italy (e-mail: facheris@ingfi1.ing.unifi.it).

Publisher Item Identifier S 0196-2892(02)04591-6.

From a practical feasibility point of view, however, some further analysis is needed. First, the choice of a transmission system directly influences the accuracy of spectral sensitivity measurements, thus the robustness to noise must be investigated. In addition to that, it is required that the noise effects on the sensitivity measurements be comparable to those due to the dynamic variations (seasonal and diurnal) of the water vapor content. If they were, this would make it arduous to exploit sensitivity measurement to retrieve information on water vapor content.

For the above reasons, in this paper we first define the structure of an attenuation measurement system that can be utilized for estimating spectral sensitivity, based on the transmission and reception of amplitude modulated signals. We present the results of performance simulations accounting for atmospheric composition, atmospheric absorption, and receiver's noise. Then, we analyze the effects on the spectral sensitivity of the variations of the water vapor profile, utilizing as reference a radiosonde data set covering a whole year of measurements on the same location. In first place, we focus on the effects of the variations of water vapor content on the range of variability of the spectral sensitivity. In second place, we analyze the correlation between the water vapor content at different atmospheric layers and the sensitivity at different frequencies.

II. Microwave Propagation Model

Let us consider a transmitter–receiver link orthogonal to the Earth surface, like that considered in [1].

Denoting with z_{tx} and z_{rx} the transmitter and receiver's positions, respectively, the power P_{rx} received in z_{rx} can be expressed as [2]

$$P_{rx}(f) = \alpha(f) P_{tx}(f) \exp(-\tau(f)) \tag{1}$$

where f is the frequency in hertz, $P_{tx}(f)$ is the transmitted spectral power, $\tau(f)$ is the optical depth accounting for atmospheric attenuation only, while $\alpha(f)$ accounts for any other attenuation contribution. $\tau(f)$ is

$$\tau(f) = \int_{z_{tx}}^{z_{rx}} k(z, f)\, dz \tag{2}$$

where $k(z, f)$ is the extinction coefficient of the atmosphere between the transmitter and the receiver, accounting for power loss between z and $z + dz$. The extinction effects are due to absorption and scattering phenomena, thus $k(z, f)$ is expressed as the sum of two contributions: the absorption coefficient $k_a(z, f)$ and the scattering coefficient $k_s(z, f)$. $k_a(z, f)$ is due to molecular absorption while $k_s(z, f)$ is due to scattering induced, for

instance, by fog, haze, and clouds. In the frequency range of interest in this work (18–22 GHz), the molecular absorption is totally due to H_2O and O_2.

Concerning the extinction properties of the atmosphere, as in [1] we used the basic equations of the Millimeter-Wave Propagation Model (MPM) for moist water developed by Liebe [3], to which the reader is referred for details. Here we simply recall that the MPM permits to compute the extinction coefficients in typical atmospheric conditions up to 130-km altitude and for $f < 1000$ GHz. The model is mainly based on O_2 and H_2O spectroscopic parameters related to absorption spectral lines up to 1000 GHz.

Only atmospheric conditions are considered, characterized by relative humidity less than 100%. Under this hypothesis, in the frequency range of interest, scattering effects are negligible. Therefore, $k(z, f)$ is obtainable by the sum of five coefficients:

- $k_{(O_2)_R}$ O_2 absorption, based on 44 spectral lines up to 834 GHz;
- $k_{(w)_R}$ water vapor absorption, based on 34 spectral lines up to 988 GHz;
- $k_{(O_2)_C}$ O_2 nonresonant absorption terms;
- $k_{(N_2)_C}$ N_2 nonresonant absorption terms;
- $k_{(w)_C}$ H_2O continuum spectrum.

The above coefficients depend on temperature, pressure, and molecular concentration of water vapor, O_2, and N_2. The basic constituents of the atmosphere, N_2 and O_2, make up 99% of the dry air contents and are uniformly mixed up to several kilometers altitude: for this reason, pressure of dry air is sufficient to derive N_2 and O_2 contents. Thus, barometric pressure, temperature, and water vapor concentration are the parameters required to compute the extinction coefficient through the MPM.

III. Sensitivity Function Definition

Let us define the spectral attenuation $A(f)$ and the sensitivity function $S(f)$ respectively as

$$A(f) = \frac{P_{tx}(f)}{P_{rx}(f)} \tag{3}$$

$$S(f) = \frac{1}{A(f)} \frac{d}{df} [A(f)]. \tag{4}$$

Substituting (1) into (3) we obtain

$$A(f) = \frac{1}{\alpha(f)} \exp(\tau(f)) \tag{5}$$

while substituting (1) into (4) and considering α independent of frequency in the range of interest, we have

$$S(f) = \frac{d}{df} [\tau(f)]. \tag{6}$$

Therefore, the sensitivity function is the spectral derivative of the optical depth. In the next section, we present a simple amplitude modulation scheme through which the spectral sensitivity function can be estimated at given frequencies.

IV. Estimating the Spectral Sensitivity Function Through Amplitude Modulation

Let us assume that the transmitted signal is a sinusoidal carrier (frequency f_0), modulated in amplitude by a sinusoidal signal (with modulating frequency $f_m \ll f_o$)

$$V_{tx}(t) = V_0[1 + m\cos(2\pi f_m t)]\cos(2\pi f_0 t) \tag{7}$$

where V_0 is the voltage amplitude and m the modulation index. Therefore, the ideal transmitted spectrum consists of three spectral lines at frequencies $f_0 - f_m$, f_0, and $f_0 + f_m$. The received ideal signal $x_{in}(t)$ is thus characterized by three spectral lines, each attenuated by the pertinent atmospheric spectral factor. Thus, posing $A_- = A(f_0 - f_m)$, $A_0 = A(f_0)$, and $A_+ = A(f_0 + f_m)$ as the atmospheric power attenuation respectively at the three aforementioned frequencies, the power of the three spectral components of the received signal is

$$\begin{aligned} P_{rx-} &= \gamma_-(A_-)^{-1}P_{tx-} \\ P_{rx0} &= \gamma_0(A_0)^{-1}P_{tx0} \\ P_{rx+} &= \gamma_+(A_+)^{-1}P_{tx+} \end{aligned} \tag{8}$$

where the corresponding attenuation coefficients γ_-, γ_+, and γ_0 account for the transmitter's and receiver's characteristics at the three frequencies, while P_{tx-}, P_{tx0}, and P_{tx+} are the average power of the three transmitted spectral components

$$\begin{aligned} P_{tx-} &= \frac{(mV_0)^2}{8} \\ P_{tx0} &= \frac{V_0^2}{2} \\ P_{tx+} &= \frac{(mV_0)^2}{8}. \end{aligned} \tag{9}$$

A simple estimate of the spectral sensitivity $S(f)$ can be provided by the incremental ratio between two attenuation measurements made at sufficiently close frequencies, namely

$$\hat{S}(f) \cong \frac{A(f + \Delta f) - A(f)}{\Delta f A(f)}. \tag{10}$$

Posing $\Delta f = f_m$ and solving (8) with respect to A_- and A_+, if $\gamma_- = \gamma_+$ from (10), we obtain the following estimate of $S(f_0)$:

$$\hat{S}(f_0) \cong \frac{P_{rx-} - P_{rx+}}{2f_m P_{rx+}}. \tag{11}$$

Therefore, by means of power measurements of the two side lines of a sinusoidally amplitude modulated signal, it is possible to obtain an estimate of the sensitivity function.

Under real conditions, noise can impair attenuation measurements and the estimate of $S(f)$. In the measurement conditions considered in this work, the dominant interference is that due to the internal noise generated at the receiver. Therefore, in the following the total signal entering the receiver is modeled as the sum of the three sinusoidal signal components and of a Gaussian white noise process. In particular, the receiver scheme of Fig. 1 can provide the estimate of $S(f)$ as given by (11). The receiver is composed by two separate branches, each of which provides

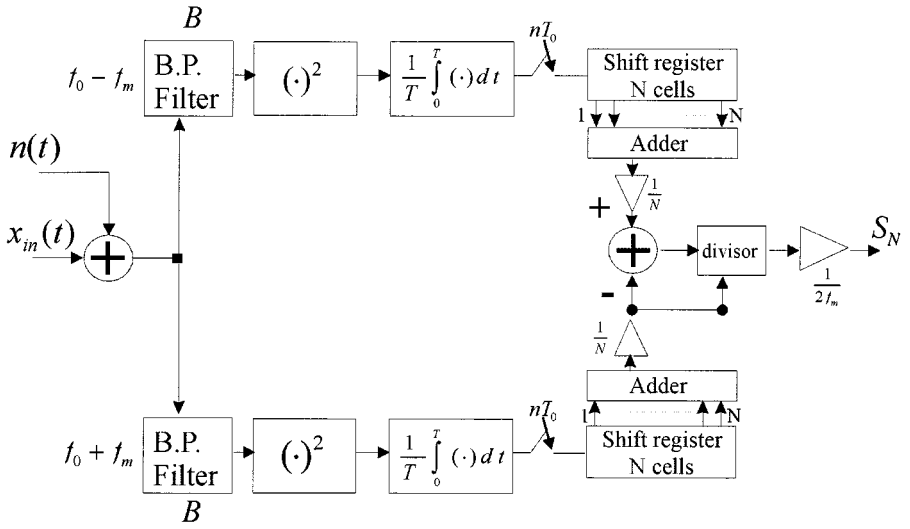

Fig. 1. Scheme of the amplitude demodulation receiving chain utilizable for sensitivity measurements.

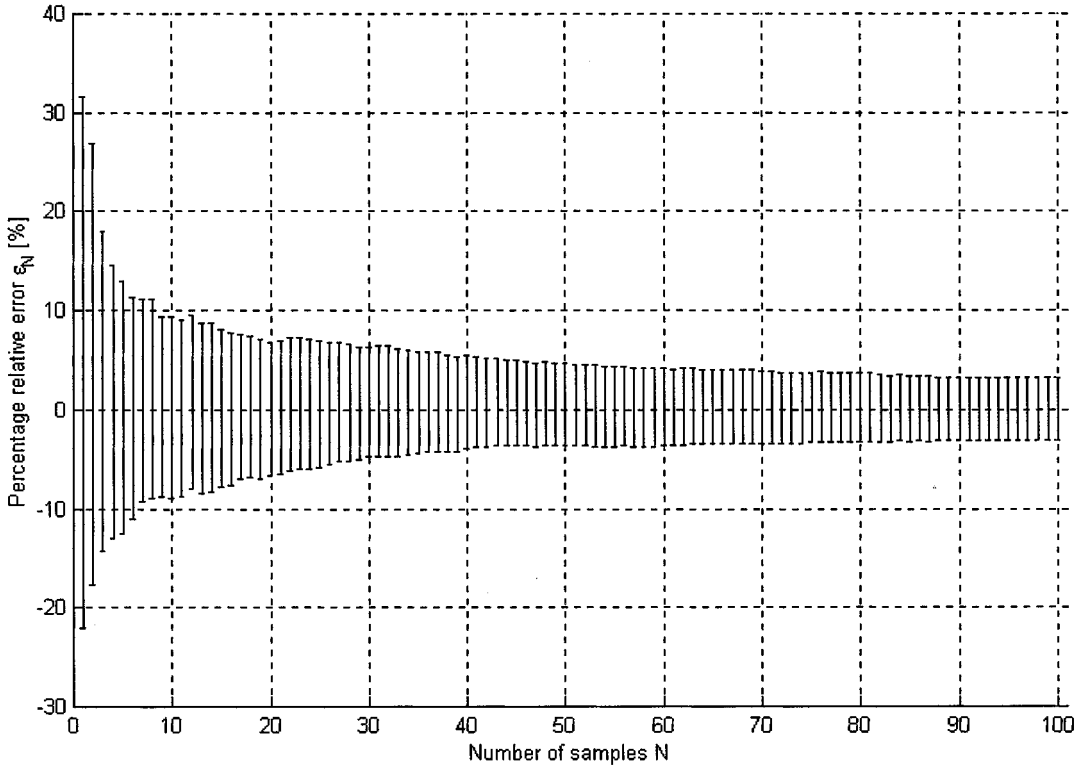

Fig. 2. Standard deviation of the error at the receiver's output (shown in Fig. 1) versus the number of integrated samples.

the power estimate of one spectral side line. On each branch, the sinusoidal signal at $f_0 - f_m$ or $f_0 + f_m$ is extracted by a band-pass filter with bandwidth B. A frequency conversion is then operated by the cascade of a memoryless device with quadratic transfer function and an integrator acting as a low-pass filter. It is thus possible to gather N estimates of the average power of the original sinusoidal oscillation of each branch by sampling the output of the integrator with sampling period T_s. Such estimates are then integrated in order to reduce the variance of the noise interference. In Fig. 1, the integration is made, on each branch, by one shift register and one adder, which provide the estimates of P_{rx-} and P_{rx+}. These are subtracted, divided by P_{rx+}, and finally multiplied by the 1/2 f_m to provide S_N, that is, the estimate of $\hat{S}$.

To analyze the errors on the estimate of $S(f)$ considering finite values of N, and different values of the involved parameters, we define $\varepsilon_N(f)$ as the percentage relative error

$$\varepsilon_N(f) = 100 \cdot \frac{S_N(f) - \hat{S}(f)}{\hat{S}(f)}. \tag{12}$$

Receiver's signal simulations have been made assuming standard power characteristics of a satellite–Earth communication

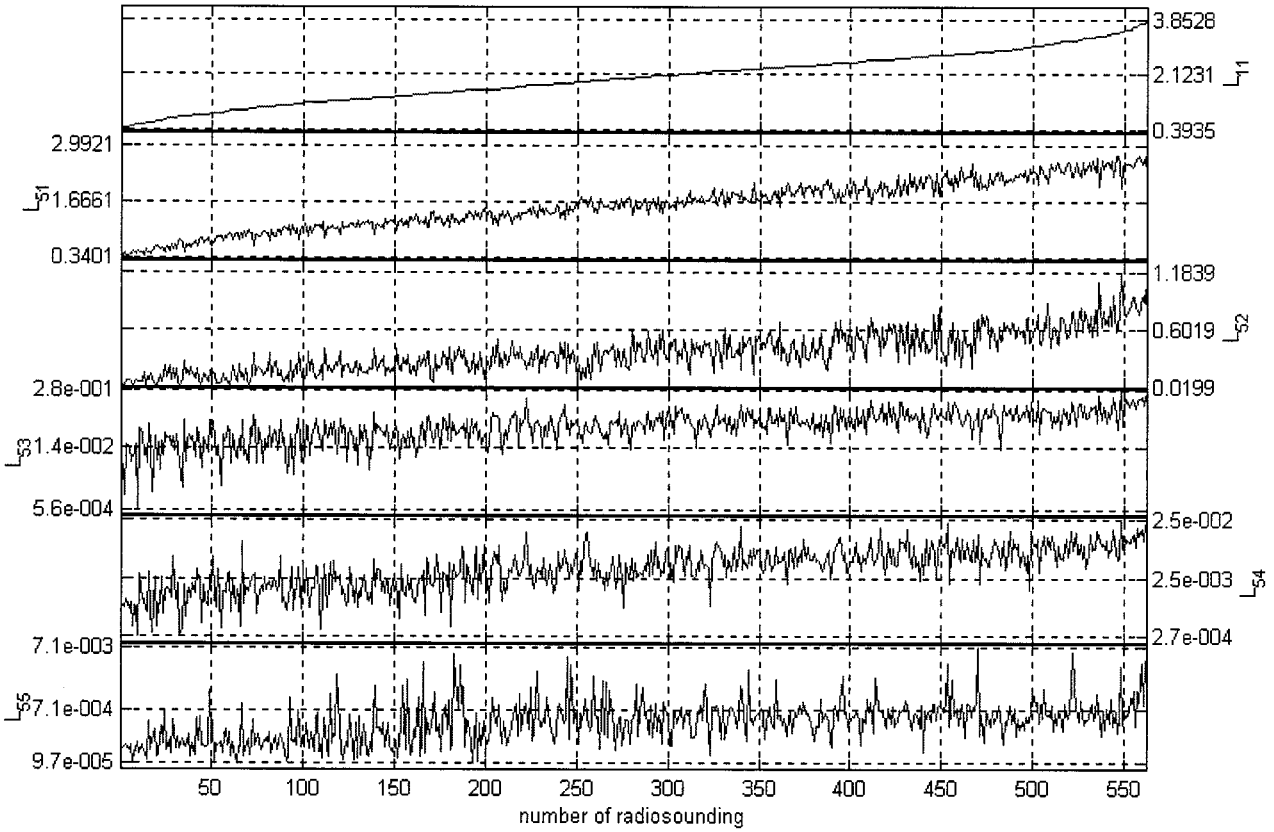

Fig. 3. Water vapor content in tropospheric layers of different thickness as derived by one year radiosonde profiles of the S. Pietro Capofiume (Bologna, Italy). Data are sorted based on growing values of the corresponding columnar water vapor content. Top to bottom: L_{11}, (0–15 km): L_{51}, (0–3 km) L_{52}, (3–6 km): L_{53}, (6–9 km): L_{54}, (9–12 km): L_{55}, (12–15 km).

link. The signal power at the receiver, excluding the attenuation effects due to the atmosphere, is

$$P_{in} = \text{EIRP} - \text{PL} + G_R \tag{13}$$

where

EIRP equivalent isotropic radiated power (in dBW);
PL propagation loss in free space (in dB);
G_R receiving antenna gain (in dB).

For a geostationary satellite, which can be considered as a worst case due to the distance involved, and for $f_0 = 20$ GHz, we have PL $= 200$ dB, EIRP $= 48$ dBW, and $G_R = 44$ dB, giving $P_{in} = -118$ dBW (about 10^{-12} W) [4]. The power spectral density of the white noise at the input of the receiver of Fig. 1 is $KT_{\text{eq}}B$ (where K is the Boltzmann's constant and T_{eq} is the receiver's equivalent temperature). The values adopted in the simulations are $T_{\text{eq}} = 195$ °K and $B = 100$ kHz; the other values we used are $m = 1$, $f_m = 100$ MHz, and $T_o = 800/f_0$.

The bar plot of Fig. 2 reports the standard deviation (estimated on 100 simulation outputs) of the error ε_N at the receiver's output for $f = 20$ GHz when varying the number of integrated samples. Notice that when $N > 50$ the standard deviation of the relative error on the estimate of $S(f)$ is lower than 5%. Under all the considered conditions, integration periods of about 10^{-6} s should be enough to provide a sufficiently accurate estimate of $\hat{S}$ at microwaves (f_0 in the range 18–22 GHz), since in such a small measurements interval the atmospheric processes involved and their parameters can be considered stationary.

V. Water Vapor Statistics

A correct and complete analysis of the correlation between $S(f)$ and the water vapor profiles must include also the knowledge of temporal variations of the water vapor content in the different tropospheric layers. In this way, it is possible to evaluate the influence of the water vapor dynamics on the measurement parameters, in particular by individuating how the variations in different atmospheric layers influence the spectral sensitivity in different frequency bands.

To this purpose, we considered the first 15 km of the atmosphere and carried out a separate analysis on n different layers of the same depth (15/n km). In the following we denote with L_{nj} ($j = 1 \cdots n$) the water vapor content of the jth layer out of n. For instance, L_{53} is the water vapor content between 6 and 9 km. Statistics were computed based on a large dataset of radiosonde data gathered at the measurement site of S. Piero Capofiume, Bologna, Italy (WMO code: 16 144). The dataset consists of 560 radiosonde profiles made throughout the whole year, accounting for all the seasonal and daily conditions. Each radiosonde profile provides vertical profiles of temperature, pressure, and relative humidity from which we obtained the profiles of water vapor.

The statistical analysis was made for different values of the number of layers n, all leading to the same conclusions. For this reason—in addition to L_{11} (the columnar water vapor content)—in the following we report only the results for $n = 5$ for each radiosonde profile, since it is the best compromise between

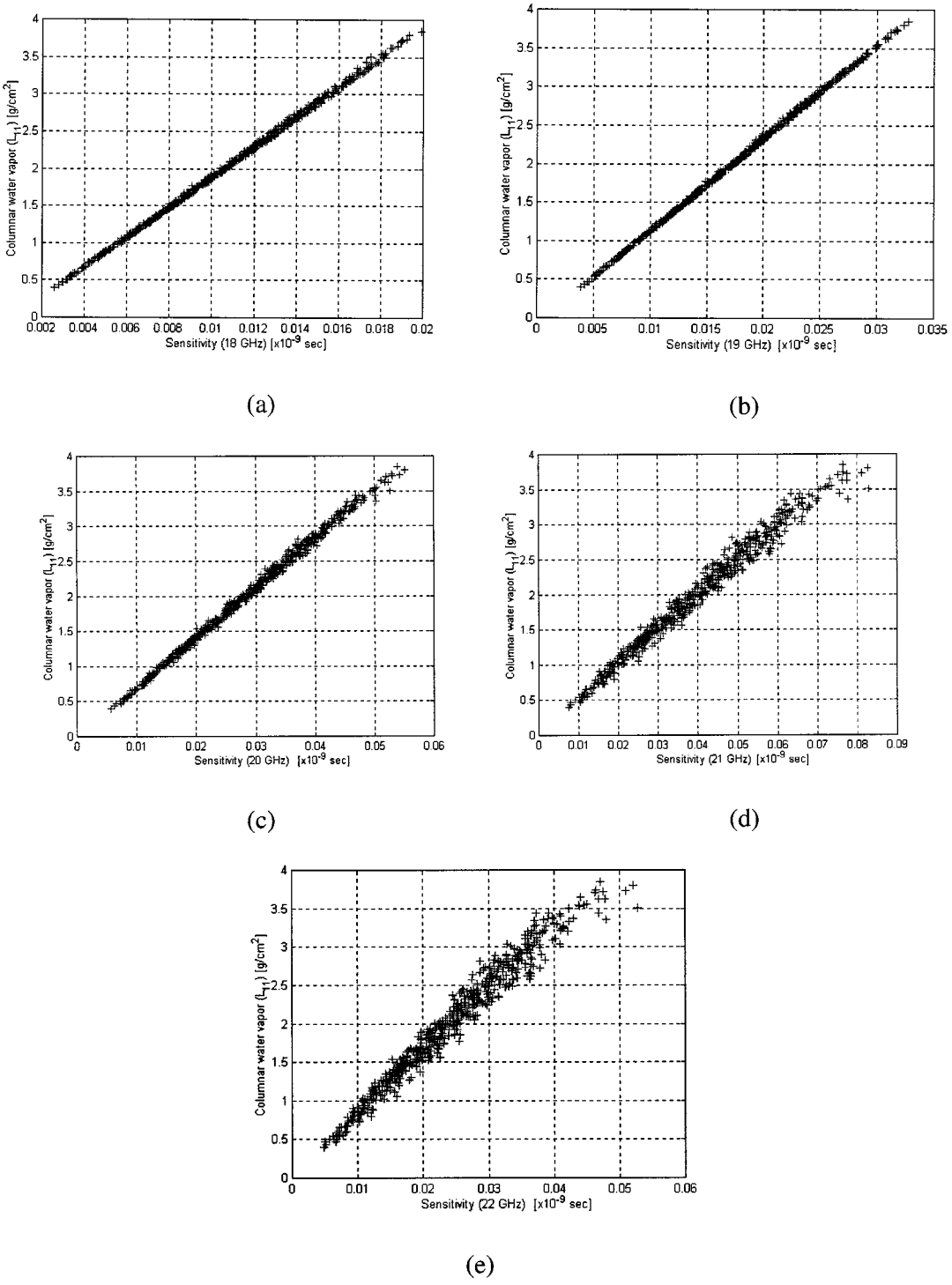

Fig. 4. Sensitivity $S(f)$ versus columnar water vapor L_{11}: (a) $f = 18$ GHz, (b) $f = 19$ GHz, (c) $f = 20$ GHz, (d) $f = 21$ GHz, and (e) $f = 22$ GHz. The sensitivity values have been obtained by simulations based on the same radiosonde data used for Fig. 1.

the opposite requirements to perform a detailed vertical analysis and to obtain a significant number of samples in every layer.

Fig. 3 reports L_{11} and all the five L_{5j} in g/cm^2. All data are shown after having sorted them by increasing values of L_{11} (so that the radiosonde profile #1 is that with the lowest columnar value). Notice that the highest and lowest values reported on the vertical axis of each plot correspond to the actual minimum and maximum of the parameter. Notice that L_{11} varies by about one order of magnitude in one year. Notice also that main contributions to L_{11} are those by L_{51} and L_{52}, whose joint effect generates the specific increasing trend of L_{11}. Also L_{53}, L_{54} and L_{55} have an increasing trend, however, though their fluctuations are bigger they do not contribute significantly to the columnar water vapor content. An important issue concerning the information carried by all L_{5j} is that, for any given small variation range of L_{11}, L_{52} can vary of more than one order of magnitude.

TABLE I
CORRELATION INDEX BETWEEN THE SENSITIVITY FUNCTION $S(f)$ AT FIVE FREQUENCIES IN THE 18–22 GHz RANGE AND THE COLUMNAR WATER VAPOR L_{11}

Frequency (GHz)	Correlation index
18	0.9996
19	**0.9998**
20	0.9980
21	0.9898
22	0.9833

VI. ANALYSIS OF THE CORRELATION BETWEEN SPECTRAL SENSITIVITY AND WATER VAPOR CONTENT

The same radiosonde data used to compute the L_{nj} parameters were exploited to simulate the attenuation effects in the measurements of $\hat{S}(f)$ made by the receiver scheme described in Section IV. Sensitivity measurements corresponding to five frequencies (18, 19, 20, 21, and 22 GHz) were simulated for each radiosonde profile. Such simulated measurements were then correlated with the columnar water vapor: Fig. 4 reports the scatter plots of sensitivity versus L_{11} for each of the five frequencies. Evidently, the linear correlation between $S(f)$ and L_{11} is remarkable for all considered frequencies (see correlation coefficients in Table I), but at 18 and 19 GHz there is—practically—a deterministic linear dependence. Moreover, at 19 GHz, the variation range of the sensitivity is greater than that at 18 GHz.

Notice that, by increasing the frequency, the variations of water vapor profiles generate increasing uncertainty on the relation between the spectral parameter and the columnar water vapor. Therefore, at 19 GHz, the columnar water vapor can be estimated quite accurately through

$$\hat{L}_{11} = a\hat{S}_{19} + b \tag{14}$$

where $\hat{L}_{11}$ is the estimate of L_{11} and $\hat{S}_{19}$ is the estimate of $S(f)$ at 19 GHz, while $a = 120.54 \cdot 10^9$ g/s·cm^2 and $b = -0.078$ g/cm^2. The high accuracy of the relationship (14) is confirmed by Fig. 5, showing L_{11} versus $\hat{L}_{11}$; the mean value and the standard deviation of the relative error are -0.01% and 0.83%, respectively.

Summarizing, sensitivity measurements made at 19 GHz can be directly exploited to provide estimates of the columnar water vapor content, while measurements made in the 20–22 GHz range cannot. However, the scatter about the regression line of Fig. 4(c)–(e) indicates that—at the parity of columnar water content—sensitivity measurements in that range depend on the specific shape of the water vapor profile. This raises the issue of determining which kind of information can be extracted from those measurements about the vertical distribution of water vapor and, since 22 GHz measurements exhibit the maximum scatter, we focused our attention on that frequency. Furthermore, as we pointed out in a recent paper, variations of water vapor content in the 3–9 km layer give the major contribution to the fluctuations sensitivity measurements in the 21–22 GHz band [1]. This implies that S_{22} [$S(f)$ for $f = 22$ GHz] can provide information about the water vapor content in that layer, whose estimate will be referred to as l_m in the following (its true value is $L_{52} + L_{53}$). Obviously, S_{22} depends on L_{11} and can therefore related to S_{19} through (14). Hence, it is reasonable to relate l_m, S_{19} and S_{22} through a linear relationship

$$l_m = cS_{19} + dS_{22}. \tag{15}$$

Using S_{19} and S_{22} obtained from radiosonde data, we got an overdetermined system of 560 linear equations from which the parameters c and d were computed by least squares fit. Their values are $c = -66.97 \cdot 10^9$ and $d = 65.88 \cdot 10^9$, both expressed in g/s·cm^2. Fig. 6 shows l_m versus $L_{52} + L_{53}$: in this case the mean value and standard deviation of the percentage relative error are 7.94% and 24.64%, respectively. Considering that the variation range of $L_{52} + L_{53}$ more than one order of magnitude, the estimate error is more than acceptable.

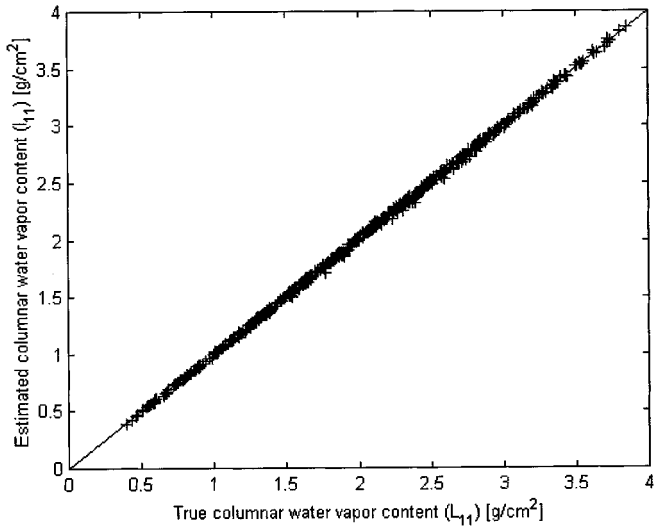

Fig. 5. The columnar water vapor content estimated by means of (14) versus the "true" one.

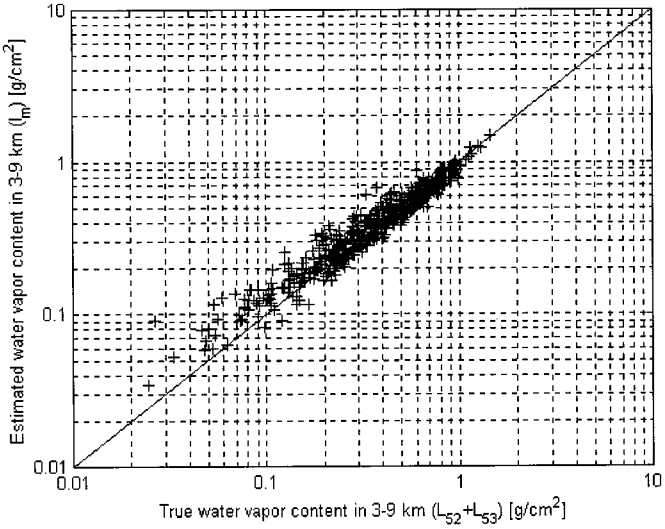

Fig. 6. The water vapor content in 3–9 km layer estimated by means of (15) versus the "true" one.

VII. Conclusion

The correlation analysis presented has confirmed that the spectral sensitivity measurement, that can be implemented by active systems, is a simple approach for providing direct information on atmospheric water vapor content. In particular, at 19 GHz, the columnar water content can be well derived directly from sensitivity, without requiring neither statistical assumption based on historic datasets nor time consuming data processing. Though accuracy is slightly worse, the same considerations hold for measurements made at 22 GHz that, once combined with those at 19 GHz, allow independent estimation of the water content in the 3–9-km layer. The two measurements can be usefully combined as constraint parameters in all procedures aiming at retrieving the water vapor profiles and at calibrating/validating radiometric measurements. Furthermore, the technology required by the implementation of the transmission/reception devices is low cost since it has been largely utilized by telecommunication systems.

Notice that the performance of the transmission/reception system have been evaluated based on parameters that are typical of a geostationary satellite. This configuration, besides representing the worst case in terms of EIRP, would guarantee continuous time monitoring of the water vapor along the selected link. Evidently, in order to provide also adequate spatial coverage and accounting for the transmit antenna characteristics, a set of ground receivers should be displaced on the areas of interest. Also, the use of Low Earth Orbiting (LEO) satellites could be envisaged, with evident benefits in terms of power requirement, but continuous time monitoring would not be possible and the time available for signal reception must be carefully accounted for in order to avoid problems due to limited accuracy in the spectral sensitivity measurements. However, a way to make the LEO configuration more profitable could be to resort to a monostatic radar system (e.g., FM-CW) by measuring the two-way differential attenuation exploiting the reflection of the ground surface in the 19–22-GHz band.

Acknowledgment

The authors are very grateful to the U.K. Meteorological Office for putting at disposal radiosonde data through its web site.

References

[1] F. Cuccoli, L. Facheris, S. Tanelli, and D. Giuli, "Microwave attenuation measurements in satellite-ground links: The potential of spectral analysis for water vapor profiles retrieval," *IEEE Trans. Geosci. Remote Sensing*, vol. 39, pp. 645–654, Mar. 2001.

[2] F. T. Ulaby, R. K. Moore, and A. K. Fung, *Microwave Remote Sensing, Cap 4*. Norwell, MA: Artech House, 1986, vol. I.

[3] H. J. Liebe, G. A. Hufford, and M. G. Cotton, "Propagation modeling of moist air and suspended water/ice particles at frequencies below 1000 GHz," presented at the AGARD Meeting on Atmospheric Propagation Effects Through Natural and Man-Made Obscurants for Visible to MM-Wave Radiation, May 1993.

[4] F. Carducci and M. Francesi, "The Italsat satellite system," *Int. J. Satellite Commun.*, vol. 13, pp. 49–81, 1995.

Fabrizio Cuccoli received the Laurea degree (cum laude) in electronic engineering from the University of Florence, Florence, Italy, in 1996 and the Ph.D. degree in "Methods and technologies for environmental monitoring" from the Università della Basilicata, Italy, in 2001.

Since 2000, he has been a Research Scientist for the Consorzio Nazionale Interuniversitario delle Telecomunicazioni (CNIT) at the Dipartimento di Elettronica e Telecomunicazioni, University of Florence, where he works together with the Radar and Radiocommunications Laboratory team. His main research activity is in the area of remote sensing of rainfall, water vapor and atmospheric gaseous components through active systems (e.g., meteorological radar, infrared and microwave devices). His current interest is the microwave and infrared spectral analysis of absorption characteristics of the atmosphere components and related data processing.

Luca Facheris received the Laurea degree (cum laude) in electronic engineering from the University of Florence, Florence, Italy, in 1989 and the Ph.D. degree in electronic and information engineering from the University of Padua, Padua, Italy, in 1993.

Since 1993, he has been an Assistant Professor in the Telecommunications area at the Department of Electronic Engineering, University of Florence. His main research activity is in the area of signal and data processing for active remote sensing: radar polarimetry, ground and spaceborne weather radars, and methods for the exploitation of attenuation measurements at microwaves and infrared for remote sensing of the atmosphere.